to $-2J$ is antiferromagnetic, and its value ranges from 2–3 cm^{-1} (as in **1**) to 590–770 cm^{-1} (as in **3**) when one acetate ligand is considered.

Conclusions

The results of these nonempirical VB calculations support the conclusion obtained from earlier MO–CI and VB studies[15] that O–O overlap within the carboxylate ligands is primarily responsible for the antiferromagnetism that is observed for Cu(II) carboxylate dimers. The resulting stabilization of the $S = 0$ state relative to the $S = 1$ state arises primarily from covalent–ionic resonance of the Pauling "3-electron bond" type, i.e., it leads to the development of this type of bond (O·O) between the oxygen atoms of the carboxylate ligands. The "cis O–O overlap" contributions to the rotation barriers for N_2O_4,[24e-h,41] N_2O_3,[41] and related molecules are also associated with the development of in-plane Pauling "3-electron bonds" between pairs of cis oxygen atoms in the planar conformers.

Acknowledgment. We thank the Australian Research Grants Scheme for financial support for this project. One of us (F.L.S.) acknowledges the award of a University of Melbourne Postgraduate Scholarship.

(41) Harcourt, R. D.; Skrezenek, F. L.; Volkoff, C., in preparation.

Electrochemical Oxidation of the Tetrakis(μ-pyrophosphito-*P*,*P*′)diplatinum(II) Complex $Pt_2(\mu\text{-}P_2O_5H_2)_4^{4-}$ Both in the Presence and the Absence of Halide Ions, and Reduction of the Axially Substituted Halodiplatinum(III) Complexes $Pt_2(\mu\text{-}P_2O_5H_2)_4X_2^{4-}$

Samuel A. Bryan, Russell H. Schmehl, and D. Max Roundhill*

Contribution from the Department of Chemistry, Tulane University, New Orleans, Louisiana 70118. *Received April 7, 1986*

Abstract: In the presence of added halide ions X^- (X = Cl, Br, I), aqueous solutions of the complex $Pt_2(\mu\text{-}P_2O_5H_2)_4^{4-}$ can be electrochemically oxidized to $Pt_2(\mu\text{-}P_2O_5H_2)_4X_2^{4-}$. Lowering the potential causes the reaction to reverse. The OTTLE cell data for all three reactions show isosbestic points and no intermediates. The potential required for the oxidation of $Pt_2(\mu\text{-}P_2O_5H_2)_4^{4-}$ and the reduction of $Pt_2(\mu\text{-}P_2O_5H_2)_4X_2^{4-}$ depends on X. By differential pulse polarography at a glassy carbon electrode the peak potential for oxidation is 0.69 V, and with added Cl^-, Br^-, and I^- the respective potentials are 0.56, 0.37, and −0.03 V vs. Ag/AgCl. The peak potentials for reduction of $Pt_2(\mu\text{-}P_2O_5H_2)_4X_2^{4-}$ for X = Cl, Br, and I are −0.11, −0.18, and −0.21 V, respectively. The complex $Pt_2(\mu\text{-}P_2O_5H_2)_4^{4-}$ reduces at a potential of −0.43 V in the presence of magnesium ion. The cyclic voltammograms in aqueous solution with added halide ion show irreversible behavior with $E_{pa} - E_{pc}$ values of 0.86, 0.65, and 0.29 V for X = Cl, Br, and I. Rapid scan (1000 V/s) cyclic voltammetry in acetonitrile solvent with no added halide ion shows irreversible behavior with oxidation and reduction waves at 1.12 and 0.61 V. The electrochemical data are explained on the basis of halide ion adsorption at the electrode surface.

The diplatinum(II) complex anion $Pt_2(\mu\text{-}P_2O_5H_2)_4^{4-}$ has attracted interest primarily because of its intense luminescence in aqueous solution at ambient temperature.[1] The ground- and excited-state chemistry of this complex can be rationalized on the basis of Gray's simplified molecular orbital model for binuclear complexes.[2] In this model the close separation between the planar d^8 metal centers causes the d_{z^2} and p_z orbitals to split into bonding and antibonding pairs. The ground-state electron configuration of $Pt_2(\mu\text{-}P_2O_5H_2)_4^{4-}$ is $d\sigma^2d\sigma^{*2}$, and the excited-state configuration is $d\sigma^2d\sigma^{*1}p\sigma^1$. Electron-transfer reactions with these two states has been the source of much interest, but there is no published work describing the electrochemistry of these complexes.

The Pt(II) complex $Pt_2(\mu\text{-}P_2O_5H_2)_4^{4-}$ will undergo two-electron oxidation to give products having Pt(III) centers. If this oxidation is effected with halogens X_2 (X = Cl, Br, I) the product is $Pt_2(\mu\text{-}P_2O_5H_2)_4X_2^{4-}$. Alternatively the oxidation can be effected with one-electron oxidants such as ceric ion or hexachloroiridate(IV). In the presence of halide ion the product is again $Pt_2(\mu\text{-}P_2O_5H_2)_4X_2^{4-}$, but with Ce^{4+} in the absence of added halide ion the complex $Pt_2(\mu\text{-}P_2O_5H_2)_4(H_2O)_2^{2-}$ is formed. In reverse, the conversion of $Pt_2(\mu\text{-}P_2O_5H_2)_4X_2^{4-}$ to $Pt_2(\mu\text{-}P_2O_5H_2)_4^{4-}$ can be accomplished by using acidified zinc, ascorbic acid, sulfite ion, or hydrogen as reductants. No intermediates have been observed in these transformations.[3] By contrast the reduction of $Pt_2(\mu\text{-}P_2O_5H_2)_4^{4-}$ to either the Pt(I,II) or the Pt(I) complexes $Pt_2(\mu\text{-}P_2O_5H_2)_4^{5-}$ and $Pt_2(\mu\text{-}P_2O_5H_2)_4^{6-}$ has been reported.[4] The former complex has been observed by pulse radiolysis techniques, and the latter anion is reported formed by the chromous ion reduction of the Pt(II,II) ground state.

Electron-transfer reactions with the excited state $Pt_2(\mu\text{-}P_2O_5H_2)_4^{4-*}$ have also been reported. Quenching studies show that this state is both a strong oxidant and reductant, and in the photoinduced addition of aryl halides to $Pt_2(\mu\text{-}P_2O_5H_2)_4^{4-}$ it has been proposed that the pathway involves an $S_{RN}1$ electron-transfer mechanism from the excited state to the aryl halide.[5] Although

(1) Sperline, R. P.; Dickson, M. K.; Roundhill, D. M. *J. Chem. Soc., Chem. Commun.* **1977**, 62–63.
(2) Mann, K. R.; Gordon, J. G., II.; Gray, H. B. *J. Am. Chem. Soc.* **1981**, *103*, 7061–7064.
(3) Bryan, S. A.; Dickson, M. K.; Roundhill, D. M. *J. Am. Chem. Soc.* **1984**, *106*, 1882–1883. Che, C.-M.; Butler, L. G.; Grunthaner, P. J.; Gray, H. B. *Inorg. Chem.* **1985**, *24*, 4662–4665.
(4) Che, C.-M.; Atherton, S. J.; Butler, L. G.; Gray, H. G. *J. Am. Chem. Soc.* **1984**, *106*, 5143–5145. Alexander, K. A.; Stein, P.; Hedden, D. B.; Roundhill, D. M. *Polyhedron* **1983**, *2*, 1389–1392.
(5) Roundhill, D. M. *J. Am. Chem. Soc.* **1985**, *107*, 4354–4356.

0002-7863/86/1508-5408$01.50/0

no electrochemical studies have been reported, several estimates of the one-electron redox potentials involved have been made. Overall these estimates suggest that the oxidation of $Pt_2(\mu\text{-}P_2O_5H_2)_4^{4-}$ requires a potential of <1.0 V, and the reduction requires a potential of −1.6 V vs. Ag/AgCl.[6]

We have now carried out electrochemical measurements with $Pt_2(\mu\text{-}P_2O_5H_2)_4^{4-}$ and find that, as expected, the redox chemistry shows irreversible behavior. We have, nevertheless, obtained measured potentials which we can relate to the known solution chemistry of these bimetallic complexes and also to the previously reported electrochemical potentials of monomeric haloplatinum(II) and (IV) complexes.

Experimental Section

The complex $K_4[Pt_2(\mu\text{-}P_2O_5H_2)_4]$ was prepared by standard procedures.[7] The PPN^+ salt was prepared by the addition of (PPN)F (PPN^+ is bis(diphenylphosphino)iminium ion) to an aqueous solution of the potassium salt. Electrochemical measurements were carried out on a PAR Model 170 electrochemical apparatus. Cells were purchased from either IBM or Bioanalytical Systems Inc. Platinum, gold, and glassy carbon disk electrodes were purchased from the latter supplier. Platinum gauze electrodes were available in our laboratories and shaped to fit the particular cell used.

An OTTLE cell was assembled by using a 1 cm × 1 cm platinum wire mesh (ca. 20 wires cm^{-1}) with a platinum wire connection sandwiched between two 1 cm × 3 cm quartz microscope slides. These slides were sealed on the vertical sides with Teflon tape, leaving the top and bottom edges open. Analyte solution was introduced into the cell by capillary action. This cell was used in conjunction with a platinum gauze auxiliary electrode and a Ag/AgCl reference electrode, the latter being placed with its Vycor tip in close proximity to the bottom opening of the OTTLE cell. The potential between the working and reference electrodes was controlled by using a variable potentiostat (BAS, CV-1B) and monitored by using a voltmeter (Danameter). The cell was mounted inside the cell compartment of a Hewlett-Packard Model 8451A diode array spectrometer, and the cell position was adjusted to obtain maximum transmittance.

Electrolyses of $Pt_2(\mu\text{-}P_2O_5H_2)_4^{4-}$ with X^- (X = Cl, Br, I) in the OTTLE cell were carried out in phosphate ion buffer at pH 6. For X = Cl and I, μ = 0.11 m and X^- = 0.01 M; and for X = Br, μ = 0.2 M and Br^- = 0.1 M. In each case a series of spectra was collected as the potential at the working electrode was scanned. The potential limits were dependent on the anion X^-; for X = Cl, Br, and I the respective voltage ranges against Ag/AgCl were −0.20 to +1.40 V, −0.25 to +0.60 V, and −0.40 to +0.35 V. The absorption band shifts were reversed by returning the potential of the working electrode to the negative limit.

In each cyclic voltammogram a "blank" voltammogram was run by using all components present other than $Pt_2(\mu\text{-}P_2O_5H_2)_4^{4-}$. Aqueous cyclic voltammograms were obtained in phosphate buffer (10 mL, μ = 1.0 M, pH 6.0) with added sodium halide (100 mM). In each case approximately 20 mg of $K_4[Pt_2(\mu\text{-}P_2O_5H_2)_4]$ was added to the solution. Each solution was purged with nitrogen for 5–10 min. The working electrode used in all cyclic voltammograms was a glassy carbon electrode. The auxiliary electrode was a platinum wire, and the scan rate ranged from 20 to 200 mV/s. Rapid scan (10–1000 V/s) cyclic voltammograms of $(C_4H_9N)_4[Pt_2(\mu\text{-}P_2O_5H_2)_4]$ in acetonitrile solvent were measured by using a PAR Model 173 Potentiostat, a PAR Model 176 current follower, and a PAR Model 175 Universal Programmer. Output of the current follower was recorded by using a Tektronix Model 390 A/D transient digitizer. Voltammograms were output to a Hewlett Packard Model 7015B x-y recorder. The cell for rapid scan cyclic voltammetric experiments consisted of a platinum bead (approximately 0.05 cm^2 area) working electrode, a platinum ring counter electrode, and an SSCE reference. All solutions were deaerated by nitrogen gas purge.

Differential pulse polarograms were measured on a PAR Model 170 apparatus by using the same solutions for oxidation as those prepared for cyclic voltammetry. For the reductions no halide ion was present, but the solution being studied contained added $MgSO_4$ (approximately 0.04 M). Data were collected at a scan rate of 5 mV/s, with a 10-mV excitation pulse, a 0.5-s "drop time", and a 10-ms sample duration. All $E_{1/2}$ values were recorded against a Ag/AgCl reference electrode. When a dropping mercury electrode (DME) was employed, the mercury capillary tube was connected to a PAR Model 172 mechanical drop timer driven by the PAR Model 170 apparatus to sequence the drop time.

(6) Heuer, W. B.; Totten, M. D.; Rodman, G. S.; Hebert, E. J.; Tracy, H. J.; Nagle, J. K. *J. Am. Chem. Soc.* **1984**, *106*, 1163–1164.
(7) Alexander, K. A.; Bryan, S. A.; Dickson, M. K.; Hedden, D.; Roundhill, D. M. *Inorg. Synth.*, **1986**, *24*, 211–213.

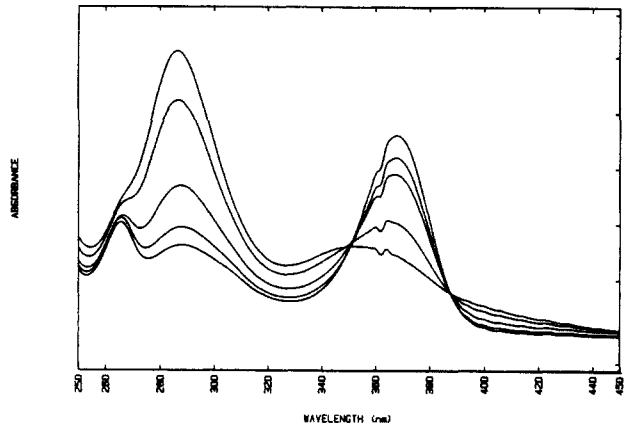

Figure 1. Spectral overlay for the interconversion between $Pt_2(\mu\text{-}P_2O_5H_2)_4^{4-}$ and $Pt_2(\mu\text{-}P_2O_5H_2)_4Cl_2^{4-}$ in an OTTLE cell ($\lambda_{max}(Pt_2(\mu\text{-}P_2O_5H_2)_4^{4-})$ = 368 nm; $\lambda_{max}(Pt_2(\mu\text{-}P_2O_5H_2)_4Cl_2^{4-})$ = 286 nm).

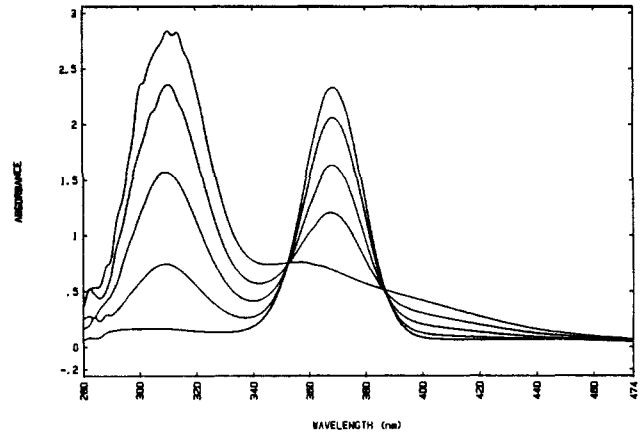

Figure 2. Spectral overlay for the interconversion between $Pt_2(\mu\text{-}P_2O_5H_2)_4^{4-}$ and $Pt_2(\mu\text{-}P_2O_5H_2)_4Br_2^{4-}$ in an OTTLE cell ($\lambda_{max}(Pt_2(\mu\text{-}P_2O_5H_2)_4^{4-})$ = 368 nm; $\lambda_{max}(Pt_2(\mu\text{-}P_2O_5H_{24}Br_2^{4-})$ = 310 nm).

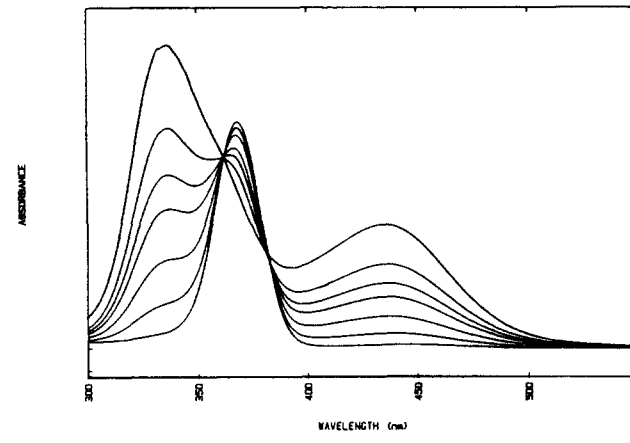

Figure 3. Spectral overlay for the interconversion between $Pt_2(\mu\text{-}P_2O_5H_2)_4^{4-}$ and $Pt_2(\mu\text{-}P_2O_5H_2)_4I_2^{4-}$ in an OTTLE cell (λ_{max} ($Pt_2(\mu\text{-}P_2O_5H_2)_4^{4-}$) = 368 nm; $\lambda_{max}(Pt_2(\mu\text{-}P_2O_5H_2)_4I_2^{4-})$ = 338 nm and 434 nm).

Results

Spectroelectrochemistry. The spectral overlays obtained in the electrochemical conversions between $Pt_2(\mu\text{-}P_2O_5H_2)_4^{4-}$ and $Pt_2(\mu\text{-}P_2O_5H_2)_4X_2^{4-}$ with added X^- are shown in Figures 1–3 where X^- = Cl^-, Br^-, and I^- (eq 1). No complexation by fluoride ion is observed; electrochemical oxidation of an aqueous solution containing $Pt_2(\mu\text{-}P_2O_5H_5)_4^{4-}$ and F^- gives only $Pt_2(\mu\text{-}P_2O_5H_5)_4(H_2O)_2^{2-}$ (λ_{max} = 248 nm).[3] The spectral data obtained in

$$Pt_2(\mu\text{-}P_2O_5H_2)_4^{4-} + 2X^- \underset{2e^-}{\overset{-2e^-}{\rightleftharpoons}} Pt_2(\mu\text{-}P_2O_5H_2)_4X_2^{4-} \quad (1)$$

Figures 1–3 have been obtained by setting the working electrode

Table I. Peak Potentials from Differential Pulse Polarograms for the Oxidation of $Pt_2(\mu\text{-}P_2O_5H_2)_4^{4-}$ Both with and without Added Halide Ion and for the Reduction of $Pt_2(\mu\text{-}P_2O_5H_2)_4X_2^{4-}$ [a]

soln components	peak potntl anodic, V	$W_{1/2}$, V	soln components	peak potntl cathodic,[b] V	$W_{1/2}$, V
$Pt_2(\mu\text{-}P_2O_5H_2)_4^{4-}$	0.69	0.13	$Pt_2(\mu\text{-}P_2O_5H_2)_4^{4-}$	-0.43[c]	0.094
$Pt_2(\mu\text{-}P_2O_5H_2)_4^{4-}/Cl^-$	0.56	0.10	$Pt_2(\mu\text{-}P_2O_5H_2)_4Cl_2^{4-}$	-0.18	0.125
$Pt_2(\mu\text{-}P_2O_5H_2)_4^{4-}/Br^-$	0.37	0.11	$Pt_2(\mu\text{-}P_2O_5H_2)_4Br_2^{4-}$	-0.21	0.113
$Pt_2(\mu\text{-}P_2O_5H_2)_4^{4-}/I^-$	-0.03	0.11	$Pt_2(\mu\text{-}P_2O_5H_2)_4I_2^{4-}$		
$Pt_2(\mu\text{-}P_2O_5H_2)_4^{4-}/F^-$	0.66, 0.84			-0.11	0.19

[a] 0.5-s "drop time", 10-ms sample duration, scan rate 5-10 mV s^{-1}, 10-50 mV pulse, phosphate buffer with μ = 1.0 M and pH 6.0, Ag/AgCl reference electrode, glassy carbon-working electrode. [b] $MgSO_4$ (50 mg) added to the solution sample containing $K_4[Pt_2(\mu\text{-}P_2O_5H_2)_4X_2]$ (20 mg). [c] Dropping mercury electrode.

at an initial low potential and then ramping the voltage to more positive potentials and holding the potential until no further spectral changes are observed. In each case the solution was buffered to a pH of 6 with phosphate buffer. The respective voltage ramps (vs. a Ag/AgCl reference electrode) for X^- = Cl^-, Br^-, and I^- are 0.2 to 1.4, -0.25 to -0.6, and -0.4 V to 0.35 V. These upper limits are set to avoid the oxidation of the halide ion X^-, since it is known that the halogens X_2 (X = Cl, Br, I) will readily add to $Pt_2(\mu\text{-}P_2O_5H_2)_4^{4-}$ to give $Pt_2(\mu\text{-}P_2O_5H_2)_4X_2^{4-}$.[8] In the spectral overlays it is clear that $Pt_2(\mu\text{-}P_2O_5H_2)_4^{4-}$ (λ_{max} = 368 nm) undergoes progressive electrochemical oxidation to $Pt_2(\mu\text{-}P_2O_5H_2)_4X_2^{4-}$ (λ_{max} = 286 nm (X = Cl), 310 nm (X = Br), 338 nm, and 434 nm (X = I)).[8] In each case two isobestic points are found, indicating that no mixed valence $Pt_2(II,III)$ intermediate $Pt_2(\mu\text{-}P_2O_5H_2)_4X^{4-}$ is formed in significant quantity during the conversion. All three conversions can be reversed by lowering the potential of the working electrode to the lower limit of the respective range. The spectral overlays are identical with those observed by anodic sweeping, and again no detectable intermediates are formed. The spectroelectrochemical oxidation and reduction data therefore correlate with the chemical results where no mixed valence intermediates are observed with one-electron oxidants and reductants, and the numbers of electrons involved in the oxidation of $Pt(\mu\text{-}P_2O_5H_2)_4^{4-}$ is two.

Although no mixed-valence intermediates are detected, these electrochemical transformations can be explained on the basis of one-electron oxidations and reductions via the unstable Pt(II,III) transient $Pt_2(\mu\text{-}P_2O_5H_2)_4X^{4-}$. This anion has been isolated and characterized in the solid state, but in aqueous solution it has been observed to rapidly disproportionate into $Pt_2(\mu\text{-}P_2O_5H_2)_4^{4-}$ and $Pt_2(\mu\text{-}P_2O_5H_2)_4X_2^{4-}$.[9] The interconversion between $Pt_2(\mu\text{-}P_2O_5H_2)_4^{4-}$ and $Pt_2(\mu\text{-}P_2O_5H_2)_4X_2^{4-}$ via the mixed valence intermediate $Pt_2(\mu\text{-}P_2O_5H_2)_4X^{4-}$ is shown in eq 2. The instability

$$2Pt_2(\mu\text{-}P_2O_5H_2)_4^{4-} \xrightarrow{-2e^-,\,2X^-} 2Pt_2(\mu\text{-}P_2O_5H_2)_4X^{4-} \longrightarrow Pt_2(\mu\text{-}P_2O_5H_2)_4^{4-} + Pt_2(\mu\text{-}P_2O_5H_2)_4X_2^{4-} \quad (2)$$
$$2Pt_2(\mu\text{-}P_2O_5H_2)_4X_2^{4-} \xrightarrow{2e^-,\,-2X^-}$$

of these one-electron oxidized intermediates to disproportionation explains our observed stoichiometric conversion between $Pt_2(\mu\text{-}P_2O_5H_2)_4^{4-}$ and $Pt_2(\mu\text{-}P_2O_5H_2)_4X^{24-}$ without any intermediates being detected.

Potential Sweep Methods. Both $Pt_2(\mu\text{-}P_2O_5H_2)_4^{4-}$ and $Pt_2(\mu\text{-}P_2O_5H_2)X_2^{4-}$ were examined by using differential pulse polarography (DPP) at both mercury and glassy carbon-working electrodes. Cathodic peak currents are observed for polarograms of $Pt_2(\mu\text{-}P_2O_5H_2)X_2^{4-}$ and anodic peaks are observed for $Pt_2(\mu\text{-}P_2O_5H_2)^{4-}$. In each case the aqueous solutions are buffered to pH 6.[10] Peak potentials and widths at half height from differential pulse measurements are listed in Table I. For reversible couples the peak potentials correspond to half wave potentials. In this case the preelectrolysis condition established in the potential ramp

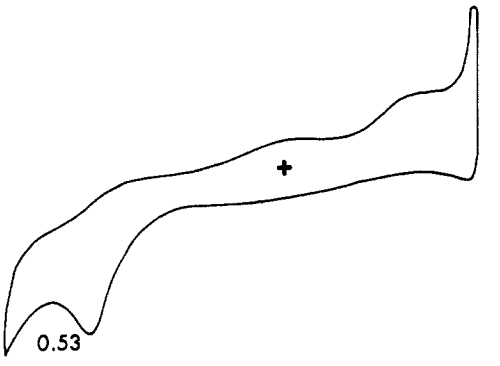

Figure 4. Cyclic voltammogram (0.10 V/s) of $Pt_2(\mu\text{-}P_2O_5H_2)_4^{4-}$ and Cl^- in aqueous solution at a glassy carbon electrode (v = 200 mV/s) (V vs. Ag/AgCl).

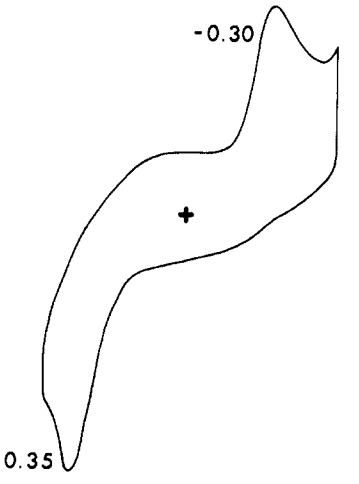

Figure 5. Cyclic voltammogram (0.10 V/s) of $Pt_2(\mu\text{-}P_2O_5H_2)_4^{4-}$ and Br^- in aqueous solution at a glassy carbon electrode (V vs. Ag/AgCl).

of the polarogram serves to deplete the analyte in the vicinity of the electrode (due to rapid disproportionation, vide infra). As a result, the peak potentials will be less positive for oxidation of $Pt_2(\mu\text{-}P_2O_5H_2)_4^{4-}$ and less negative for reduction of $Pt_2(\mu\text{-}P_2O_5H_2)X_2^{4-}$ than potentials expected for the reversible one-electron process. The value of the polarographic measurements in this work relates to the widths, $W_{1/2}$, of the DPP waves, which are a measure of the kinetic reversibility of the heterogeneous electron transfer. For a one-electron process at the electrode the limiting $W_{1/2}$ value is 90 mV,[11] and $W_{1/2}$ increases as the charge transfer becomes irreversible. For the complexes examined, only $Pt_2(\mu\text{-}P_2O_5H_2)_4Cl_2^{4-}$ exhibits a $W_{1/2}$ suggesting significant charge-transfer irreversibility. Provided the electrode process is a single electron transfer, the results indicate that electron transfer between the glassy carbon-working electrode and the complexes is facile. The large peak potential differences observed for $Pt_2(\mu\text{-}P_2O_5H_2)_4^{4-}$ in the presence of different halides are discussed below.

(8) Che, C.-M.; Schaefer, W. P.; Gray, H. B.; Dickson, M. K.; Stein, P. B.; Roundhill, D. M. *J. Am. Chem. Soc.* **1982**, *104*, 4253-4255.
(9) Che, C.-M.; Herbstein, F. H.; Schaefer, W. P.; Marsh, R. E.; Gray, H. B. *J. Am. Chem. Soc.* **1983**, *105*, 4604-4607.
(10) Bryan, S. A., Ph.D. Thesis, Washington State University, 1985.
(11) Bard, A. J.; Faulkner, L. *Electrochemical Methods*; Wiley: New York, 180; p 149.

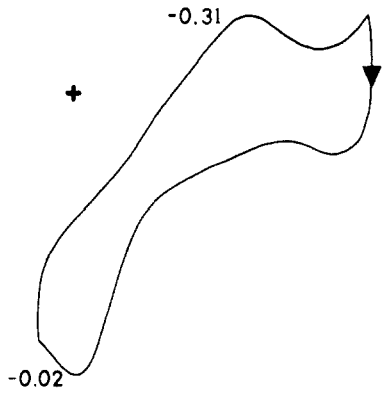

Figure 6. Cyclic voltammogram (0.10 V/s) of $Pt_2(\mu\text{-}P_2O_5H_2)_4^{4-}$ and I^- in acetonitrile at a glassy carbon electrode (V vs. Ag/AgCl).

Table II. Peak Potentials from Cyclic Voltammograms of $Pt_2(\mu\text{-}P_2O_5H_2)_4^{4-}$ in Aqueous Solutions with Added Halide Ions[a]

halide	E_{pa}, V	E_{pc}, V	$E_{pa} - E_{pc}$, V
Cl^-	0.53	−0.33	0.86
Br^-	0.35	−0.30	0.65
I^-	−0.02	−0.31	0.29

[a] Glassy carbon-working electrode, platinum wire auxiliary electrode, Ag/AgCl reference, rate = 100 mV/s, μ = 1.0 M.

Cyclic voltammograms of $Pt_2(\mu\text{-}P_2O_5H_2)_4^{4-}$ were obtained both in aqueous solution using a glassy carbon-working electrode and in acetonitrile using a platinum bead electrode. no waves were observed for the complex oxidation or reduction in aqueous solution when platinum or gold were used as working electrodes. Typical voltammograms in aqueous solution with added X^- (X = Br, Cl, I) are shown in Figures 4–6. In the absence of halide, no waves are observed at potentials between the anodic and cathodic limits of the solution. Voltammograms of $Pt_2(\mu\text{-}P_2O_5H_2)X_2^{4-}$ (X = Cl, Br, I) in aqueous solutions exhibit cathodic peaks at potentials close to those observed in voltammograms of $Pt_2(\mu\text{-}P_2O_5H_2)_4^{4-}$ in solutions containing the respective halides, after sweeping the potential past the anodic wave. In solutions containing X^- (X = Cl, Br, I), no cathodic wave is observed for $Pt_2(\mu\text{-}P_2O_5H_2)_4^{4-}$ in the first cycle when the potential is first swept from 0.0 to −0.4 V and then to positive potentials. Thus the cathodic waves observed in voltammograms of $Pt_2(\mu\text{-}P_2O_5H_2)_4^{4-}$ correspond to reduction of $Pt_2(\mu\text{-}P_2O_5H_2)X_2^{4-}$ formed upon sweeping through the anodic wave. The most striking feature of Figures 4–6 is the marked dependence of the anodic peak potential on the particular halide in solution (Table II).[12] In a series of papers Hubbard has shown that the halide dependence of peak potentials for oxidation of monomeric Pt(II) complexes can be attributed to the necessity of the halide to serve as a bridge for electron transfer between the Pt(II) complex and the electrode.[13] In this case the dependence of E_{pa} on the nature of the added halide can be attributed to a preequilibrium involving the formation of $Pt_2(\mu\text{-}P_2O_5H_2)_4X^{5-}$ at the electrode surface prior to oxidation of the complex.

Further information on the redox behavior of $Pt_2(\mu\text{-}P_2O_5H_2)_4^{4-}$ in the absence of halide is obtained from cyclic voltammograms of the Bu_4N^+ and PPN^+ salts in acetonitrile solvent. Figure 7 shows a typical voltammogram when a freshly polished platinum disk electrode is used as working electrode. A single anodic peak is observed at +0.78 V vs. SSCE, and the peak potential is independent of sweep rate (±0 mV) between 20 and 200 mV/s. This independence of E_{pa} on ν is consistent with a preequilibrium prior

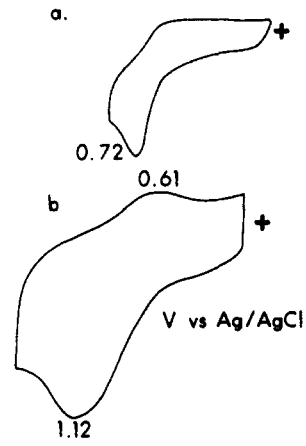

Figure 7. Cyclic voltammogram of $Pt_2(\mu\text{-}P_2O_5H_2)_4^{4-}$ in acetonitrile solution at a platinum bead electrode at sweep rates of (a) 0.20 V/s and (b) 1000 V/s.

to the redox event (i.e., a C_rE_r process in the diffusion zone, DP);[14] in this case formation of an axial solvent complex, $Pt_2(\mu\text{-}P_2O_5H_2)_4(CH_3CN)^{4-}$, is the likely preequilibrium process. Rapid scan cyclic voltammetry of $Pt_2(\mu\text{-}P_2O_5H_2)_4^{4-}$ at a platinum bead shows evidence of a small cathodic wave (E_{pc} = +0.61 V) upon reversal of the potential sweep at potentials positive of the anodic wave with a sweep rate of 1000 V/s. The midpoint between the potentials is 0.86 V vs. Ag/AgCl. The large positive shift in E_{pa} from 0.72 V at 0.2 V/s to 1.12 V at 1000 V/s results principally from a large increase in uncompensated resistance. Independent measurement of the disproportionation rate of the mixed valence Pt(II,III) complex $Pt_2(\mu\text{-}P_2O_5H_2)_4^{3-}$ prepared by pulse radiolysis gives a second-order rate constant of 6.7×10^{-8} M^{-1} s^{-1}.[15] The small relative currents observed for the cathodic wave at +0.65 V are consistent with the electrode process being one-electron reduction of $Pt_2(\mu\text{-}P_2O_5H_2)_4S^{3-}$ (S = solvent) that has not disproportionated (Figure 7). Thus the above midpoint potential of 0.86 V vs. Ag/AgCl may serve as an estimate of E° for the reversible couple shown below (eq 3).

$$Pt_2(\mu\text{-}P_2O_5H_2)_4(S)^{3-} \underset{-e^-}{\overset{+e^-}{\rightleftharpoons}} Pt_2(\mu\text{-}P_2O_5H_2)_4(S)^{4-} \qquad (3)$$

Discussion

The redox behavior of both $Pt_2(\mu\text{-}P_2O_5H_2)_4^{4-}$ and $Pt_2(\mu\text{-}P_2O_5H_2)_4X_2^{4-}$ in both aqueous solutions and acetonitrile exhibit chemical irreversibility. The heterogeneous one-electron oxidation of $Pt_2(P_2O_5H_2)_4^{4-}$ appears electrochemically reversible based upon differential pulse polarographic data. The chemical reaction following oxidation of $Pt_2(P_2O_5H_2)_4^{4-}$ is rapid, and cyclic voltammograms at 1000 V/s exhibit only partial reversibility. The observed behavior in the cyclic voltammograms qualitatively agrees with rates obtained in pulse radiolysis studies of the disproportionation of $Pt(\mu\text{-}P_2O_5H_2)_4^{3-}$ in aqueous solution. The midpoint potential (0.86 V) of the cyclic voltammogram at 1000 V/s, may be used in approximation of the excited-state oxidation potential for $Pt_2(\mu\text{-}P_2O_5H_2)_4^{4-}$, (eq 4), assuming that the entropy for re-

$$Pt_2(\mu\text{-}P_2O_5H_2)_4^{4-*} \rightarrow Pt_2(\mu\text{-}P_2O_5H_2)_4^{3-} + e^- \qquad (4)$$

organization of the excited state is small.[6,16] The potential of 1.6 ± 0.2 V thus determined accounts for the strong reducing ability of excited $Pt_2(\mu\text{-}P_2O_5H_3)_4^{4-}$ exhibited in its $S_{RN}1$ reactivity with aryl halides and is also consistent with the approximation of Gray et al. based upon luminescence quenching experiments

(12) These potentials in the presence of halide ion are not the thermodynamic potential for the oxidation of $Pt_2(\mu\text{-}P_2O_5H_2)_4^{4-}$.

(13) Cushing, J. P.; Hubbard, A. T. *J. Electroanal. Chem. Interfacial Electrochem.* **1969**, *23*, 183–203. Lau, A. L. Y.; Hubbard, A. T. *J. Electroanal. Chem. Interfacial Electrochem.* **1971**, *33*, 77–93. Lai, C.-N.; Hubbard, A. T. *Inorg. Chem.* **1974**, *13*, 1199–1204. Leban, M. A.; Hubbard, A. T. *J. Electroanal. Chem.* **1976**, *74*, 253–275. Lane, R. F.; Hubbard, A. T. *J. Phys. Chem.* **1977**, *81*, 734–739.

(14) Reference 11, p 443.

(15) Roundhill, D. M.; Atherton, S. J., submitted for publication. If we assume complete oxidation of $Pt_2(\mu\text{-}P_2O_5H_2)_4^{4-}$ to $Pt_2(\mu\text{-}P_2O_5H_2)_4^{3-}$ in the vicinity of the electrode, we can estimate that $Pt_2(\mu\text{-}P_2O_5H_2)_4^{3-}$ will have a $t_{1/2}$ of 10–100 μs.

(16) Fordyce, W. A.; Brummer, J. G.; Crosby, G. A. *J. Am. Chem. Soc.* **1981**, *103*, 7061–7064. Rice, S. F.; Gray, H. B. *J. Am. Chem. Soc.* **1983**, *105*, 4571–4575.

with a variety of electron acceptors.[17]

Reduction of $Pt_2(\mu\text{-}P_2O_5H_2)_4X_2^{4-}$ in aqueous solution results in complete conversion to $Pt_2(\mu\text{-}P_2O_5H_2)_4^{4-}$ as evidenced by spectroelectrochemical measurements. Reduction of $Pt_2(\mu\text{-}P_2O_5H_2)_4^{4-}$ itself in a solution containing magnesium ion and buffering to pH 6 shows, by differential pulse polarography, a peak at −0.43 V.[18] This observed potential supports the suggestion that $Pt_2(\mu\text{-}P_2O_5H_2)_4^{4-}$ can be reduced in aqueous solution by added chromous ion.[4] Nevertheless, the value of the potential is considerably less negative than the suggested potential of −1.4 V deduced from the oxidative quenching of $Pt_2(\mu\text{-}P_2O_5H_2)_4^{4-*}$ by amines.[6] The reduction of $Pt_2(\mu\text{-}P_2O_5H_2)_4^{4-}$ in aqueous solution remains therefore an unresolved problem, and the reason for discrepancy between these values of the potential is unclear. We must, nevertheless, emphasize that the observed reduction potential is not a thermodynamic potential since Mg^{2+} ion is intimately involved with the complex being reduced.

(17) Nocera, D. G.; Maverick, A. W.; Winkler, J. R.; Che, C.-M.; Gray, H. B. *ACS Symp. Ser.*, **1983**, *211*, 21-33.

(18) At more negative potentials we observe a large peak due to the reduction to hydrogen.

Acknowledgment. We thank Mark Dickson and Ken Alexander for preliminary electrochemical experiments. Acknowledgment is made to the donors of the Petroleum Research Fund administered by the American Chemical Society, for the support of this research (Grant No. 16965-AC3).

Scaling All Correlation Energy in Perturbation Theory Calculations of Bond Energies and Barrier Heights

Mark S. Gordon*† and Donald G. Truhlar

Contribution from the Department of Chemistry and Supercomputer Institute, University of Minnesota, Minneapolis, Minnesota 55455. *Received February 28, 1986*

Abstract: We present and test a new method for scaling all correlation energy as estimated by Møller–Plesset many-body perturbation theory with popular basis sets. Scale factors that may be useful for future applications are estimated from known bond dissociation energies. We also use scale factors to estimate the barrier heights for two hydrogen-transfer reactions, $CH_3 + H_2 \rightleftharpoons CH_4 + H$ and $OH + CH_4 \rightleftharpoons H_2O + CH_3$.

I. Introduction

Ab initio electronic structure calculations are improving steadily in accuracy and usefulness.[1] Nevertheless, in many cases, implicit and explicit extrapolation and correction schemes are needed and are used to obtain useful accuracy with lower levels of theory than would be required with unextrapolated results. An example of an implicit extrapolation scheme is the widely used assumption that errors are constant across a potential energy surface. This is equivalent to assuming that the extrapolated value E_e of the accurate (exact) total energy is given in terms of the calculated value E_c by

$$E_e = E_c + C \tag{1}$$

where C is a constant for a given reaction, i.e., C is independent of geometry and/or bond rearrangement. This assumption has proved particularly accurate when applied only to reactants and products of isodesmic or isogyric reactions,[2] but it is often applied, for lack of a better assumption, to more general reactions and to transition states. Notice of course that C need never be specified if only energy differences are considered. Another form of extrapolation, applicable only for perturbation theory, is the use of Padé extrapolants[3] to estimate the infinite-order correlation limit for a given one-electron basis set. The closest analogue for configuration-interaction-based methods is the use of threshold selection and increasingly large reference spaces to estimate the complete configuration interaction limit for a given one-electron basis.[4] Unfortunately the effects of incompleteness of the one-electron basis set are often larger than the neglect of higher order correlation effects. The method of scaled external correlation (SEC)[5] attempts to extrapolate to the full-CI limit and the complete one-electron-basis-set limit in a single step. The SEC method is based on combining the results of two ab initio calculations: a multi-configuration self-consistent-field (MCSCF)[6] calculation that accounts for specific geometry-dependent correlation effects and a multi-reference configuration interaction (MR-CI)[7] calculation that accounts for an appreciable fraction of the external (or dynamical) correlation. Then the accurate energy is approximated by[5]

$$E_{SEC} = E_{MCSCF} + \frac{E_{MRCI} - E_{MCSCF}}{\mathcal{F}} \tag{2}$$

where $\mathcal{F}$ is assumed constant, i.e., independent of geometry and/or bond rearrangement for a given system. When the one-electron basis set is very extensive, the MCSCF calculation is a full-valence

† Visiting Fellow, Minnesota Supercomputer Institute, 1985–1986. Permanent address: Department of Chemistry, North Dakota State University, Fargo, ND 58105-5516.

(1) See, e.g.: Čarsky, P.; Urban, M. *Ab Initio Calculations*; Springer: New York, 1980; *Comparison of Ab Initio Quantum Chemistry with Experiment for Small Molecules*; Bartlett, R. J., Ed.; Reidel: Dordrecht, 1985.

(2) Hehre, W.; Ditchfield, R.; Radom, L.; Pople, J. A. *J. Am. Chem. Soc.* **1970**, *92*, 4796. Hehre, W. J. *Acc. Chem. Res.* **1976**, *9*, 399. Pople, J. A.; Frisch, M. J.; Luke, B. T.; Binkley, J. S. *Int. J. Quantum Chem. Symp.* **1983**, *17*, 307. See also: Wiberg, K. B. *J. Comput. Chem.* **1984**, *5*, 197. Ibrahim, M. R.; Schleyer, P. v. R. *J. Comput. Chem.* **1985**, *6*, 157.

(3) Bartlett, R. J.; Shavitt, I. *Chem. Phys. Lett.* **1977**, *50*, 190. Purvis, G. D.; Bartlett, R. J. *J. Chem. Phys.* **1981**, *75*, 1284. Duchovic, R. J.; Hase, W. L.; Schlegel, H. B.; Frisch, M. J.; Ragavachari, K. *Chem. Phys. Lett.* **1982**, *89*, 120. Handy, N. C.; Knowles, P. J.; Somasundran, K. *Theor. Chim. Acta* **1985**, *68*, 87.

(4) Bruna, P. J.; Peyerimhoff, S. D.; Buenker, R. J. *Chem. Phys. Lett.* **1980**, *72*, 278. Buenker, R. J.; Peyerimhoff, S. D. In *New Horizons of Quantum Chemistry*; Löwdin, P.-O., Pullman, B., Eds.; Reidel, Dordrecht: Holland, 1983; p 183. Phillips, R. A.; Buenker, R. J.; Bruna, P. J.; Peyerimhoff, S. D. *Chem. Phys.* **1984**, *84*, 11.

(5) Brown, F. B.; Truhlar, D. G. *Chem. Phys. Lett.* **1985**, *117*, 307.

(6) Roos, B. O. In *Methods in Computational Molecular Physics*; Diercksen, G. H. F., Wilson, S., Eds.; Reidel: Boston, 1983; p 161.

(7) Shavitt, I. In *Advanced Theories and Computational Approaches to the Electronic Structure of Molecules*; Dykstra, C. E., Ed.; Reidel: Boston, 1984; p 185.

0002-7863/86/1508-5412$01.50/0